RESEARCH ARTICLE | JANUARY 11 2011

# Distinguishing magnetic blocking and surface spin-glass freezing in nickel ferrite nanoparticles

K. Nadeem; H. Krenn; T. Traussing; I. Letofsky-Papst



*J. Appl. Phys.* 109, 013912 (2011)
https://doi.org/10.1063/1.3527932

# Distinguishing magnetic blocking and surface spin-glass freezing in nickel ferrite nanoparticles

K. Nadeem,[1,a)] H. Krenn,[1] T. Traussing,[2] and I. Letofsky-Papst[3]
[1]*Institute of Physics, Karl-Franzens University Graz, Universitätsplatz 5, A-8010 Graz, Austria*
[2]*Institute of Materials Physics, University of Technology Graz, A-8010 Graz, Austria*
[3]*Institute for Electron Microscopy, University of Technology Graz, Steyrergasse 17, A-8010 Graz, Austria*

(Received 20 September 2010; accepted 14 November 2010; published online 11 January 2011)

Nickel ferrite nanoparticles dispersed in $SiO_2$ matrix have been synthesized by sol-gel method. Structural analysis has been performed by using x-ray diffraction and transmission electron microscopy. Magnetic properties have been investigated by using superconducting quantum interference device magnetometry. In addition to the average blocking temperature peak at $T_B = 120$ K measured by a zero field cooled temperature scan of the dc susceptibility, an additional hump near 15 K is observed. Temperature dependent out-of-phase ac susceptibility shows the same features: one broad peak at high temperature and a second narrow peak at low temperature. The high temperature peak corresponds to magnetic blocking of individual nanoparticles, while the low temperature peak is attributed to surface spin-glass freezing which becomes dominant for decreasing particle diameter. To prove the dynamics of the spin (dis)order in both regimes of freezing and blocking, the frequency dependent ac susceptibility is investigated under a biasing dc field. The frequency shift in the "frozen" low-temperature ac susceptibility peak is fitted to a dynamic scaling law with a critical exponent $zv = 7.5$, which indicates a spin-glass phase. Exchange bias is turned on at low temperature which signifies the existence of a strong core-shell interaction. Aging and memory effects are further unique fingerprints of a spin-glass freezing on the surface of isolated magnetic nanoparticles. © *2011 American Institute of Physics*. [doi:10.1063/1.3527932]

## I. INTRODUCTION

The magnetic phases of surface and core spins of small-sized nanomagnets are in the focus of current intense research. The magnetic order of the surface spins of a nanoparticle influences substantially the magnetic properties of the entire particle.[1,2] Magnetic anisotropy, saturation moment, and relaxation dynamics of individual nanoparticles are modified at low temperature.[3–5] In ferrite nanoparticles, surface disorder is more prominent due to bond frustration of the exchange interaction between ferrimagnetically coupled spins of different sublattices near the surface.[6] As the particle size is reduced, disorder and frustration at the nanoparticle's surface becomes progressively dominant with a tendency to form a spin-glass phase. Experimentally it is not easy to distinguish between the thermally activated magnetic blocking of the compact core spin moment and the freezing of disordered individual surface spins. Kodama *et al.*[7] have proposed a model for disorder-induced surface spin freezing in nickel ferrite nanoparticles. Like in bulk spin-glasses, disorder and frustration on the surface of fine nanoparticles are necessary prerequisites for a possible spin-glass freezing.[8] Winkler *et al.*[9] have recently reported spin-glass behavior in nickel oxide (NiO) nanoparticles, Peddis *et al.*[10] in fine cobalt ferrite ($CoFe_2O_4$) nanoparticles and attributed the observed spin-glass phase to a random freezing of surface spins. In this article, we will discuss the competition between magnetic blocking and surface spin-glass freezing in nickel ferrite nanoparticles dispersed in $SiO_2$ matrix. The results can be viewed as representative also for other particles with a similar size dependent bond-disorder like for antiferromagnetic particles (NiO, CoO).

## II. EXPERIMENT

Nickel ferrite nanoparticles dispersed in $SiO_2$ matrix have been synthesized by sol-gel method. The synthesis process is described in our recently published article.[11] The as-prepared samples were annealed at 900 °C. Average particle size is controlled by changing the $SiO_2$ concentration and the annealing time. Initial structural phase constitution was identified by x-ray diffraction (XRD) (Bruker D8 Advance instrument) using Cu $K_\alpha$ ($\lambda = 0.154$ nm) radiation at ambient temperature. Magnetic measurements were taken by using a superconducting quantum interference device (SQUID)-magnetometer (Quantum Design, MPMS-XL-7) with a maximum applied field of ±7 T and temperature control from 4.2 to 350 K. Transmission electron microscopy (TEM) was used (Model CM20 from FEI with 200 kV acceleration voltage and $LaB_6$ cathode) to analyze the average particle size. Surface spin-glass freezing and magnetic blocking is studied in particles of the size range 8–27 nm (evaluated by XRD). The size is controlled by variation in the $SiO_2$ content and annealing time, e.g., *8 nm particle size* sample is prepared with 70% $SiO_2$ matrix just burned at 900 °C, *12 nm particle size* sample with 70% $SiO_2$ matrix annealed at 900 °C for 2 h, *16 nm particle size* sample with 60% $SiO_2$ matrix annealed at 900 °C for 2 h, *27 nm particle size* sample with 25% $SiO_2$ matrix annealed at 900 °C for 2 h. In the following, we designate the samples *PS-8 nm*, *PS-12 nm*,

a)Electronic mail: kashif.nadeem@edu.uni-graz.at.



 

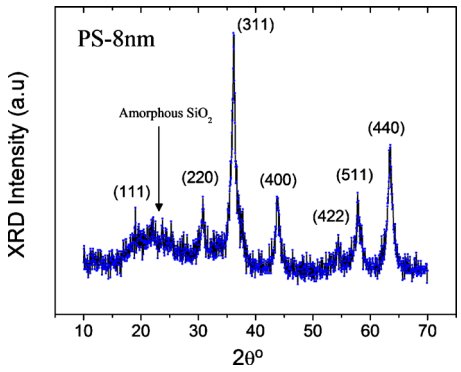


FIG. 1. (Color online) XRD pattern of sample *PS-8 nm*. A broad maximum indicated by an arrow is due to amorphous $SiO_2$ matrix.

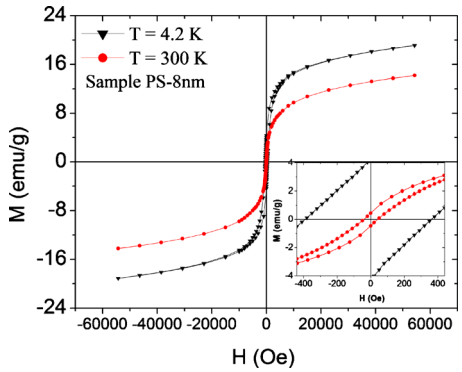


FIG. 3. (Color online) Hysteresis loops of sample *PS-8 nm* at 300 and 4.2 K. Inset: detailed coercivity ($H_c$) region of both hysteresis loops.

*PS-16 nm*, *and PS-27 nm* corresponding to the *8 nm particle size sample*, *12 nm particle size sample*, *16 nm particle size sample*, and *27 nm particle size sample*, respectively.

## III. RESULTS AND DISCUSSION

Figure 1 shows the XRD of the sample *PS-8 nm*. The identified sharp Bragg peaks are attributed to the spinel structure of nickel ferrite, which are superimposed on a broad scattering background from the amorphous $SiO_2$ matrix. Debye–Scherrer's analysis gives an average particle size of 8 nm. Figure 2(a) shows the TEM of a selected area of sample *PS-8 nm* (10 nm scale). Particles are nearly spherical in shape. Figure 2(b) zooms into the rectangle depicted in Fig. 2(a) magnifying up to the 5 nm scale. The diffraction spots located along the selected area electron diffraction (SAED) rings indicate the crystalline quality of the nanoparticles.

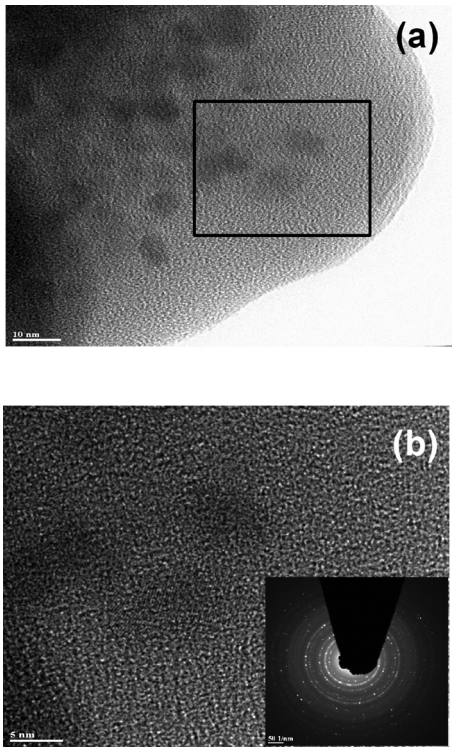


FIG. 2. (a) TEM of sample *PS-8 nm* at 10 nm scale. (b) Zoom view of rectangle as drawn in Fig. 2(a) at 5 nm scale, inset shows the SAED which indicates that nanoparticles are in crystalline form.

Magnetic measurements were taken by using a SQUID-magnetometer with maximum applied field of ±7 T and a temperature variation in the range 4.2–350 K. Frequency dependent ac susceptibility measurements were also performed by the SQUID-magnetometer in the frequency range 0.1–1000 Hz. Figure 3 shows the hysteresis loops at 300 and 4.2 K of sample *PS-8 nm* exposed to a maximum applied field of ±5.5 T. The measured coercivities ($H_c$) are 41 Oe and 375 Oe at 300 and 4.2 K, respectively (see the inset of Fig. 3). At low temperatures (<15 K) surface spins are frozen in random disorder but experience strong interactions with the ordered core spins. This core-shell interaction causes a large value of coercivity ($H_c$) at low temperature (4.2 K). Saturation magnetization ($M_s$) comes out to be 14.2 emu/g and 19.1 emu/g at 300 K and 4.2 K, respectively. At both temperatures, saturation magnetization is less than the saturation magnetization of bulk nickel ferrite: $M_s$ (bulk) =56 emu/g.[12,13] Size-dependent reduction in saturation magnetization is typical for ferrite nanoparticles and is attributed to spin-canting of surface spins.[7] The increase in $M_s$ at 4.2 K is due to a decrease in thermal fluctuations of magnetic moments.

Average blocking temperature ($T_B$) of the nanoparticles can be found from the maximum of zero field cooled (ZFC) susceptibility. Figure 4(a) displays the ZFC measurement of the sample *PS-8 nm* in the temperature range 4.2–350 K under applied field H=150 Oe. In a ZFC measurement first the sample is cooled in zero magnetic field from room temperature to 4.2 K. After cooling, a field of H=150 Oe is applied and magnetic moment is recorded with increasing temperature. There is a broad maximum at around 120 K which is interpreted as average magnetic blocking temperature ($T_B$) of the nanoparticles. Apart from this blocking peak, there is an irregularity at low temperatures in the form of a hump as indicated by the rectangle in Fig. 4(a).[14]

To investigate in detail the origin of this irregularity or hump, we have performed ac susceptibility measurements in the temperature range 4.2–350 K. Figure 4(b) shows the out-of-phase ac susceptibility of sample *PS-8 nm* with ac field modulation at frequency f=10 Hz and with field amplitude A=2 Oe. The $\chi''$(T)-plot shows two maxima, one at high temperature $T_B$=271 K and one at low temperature $T_s$

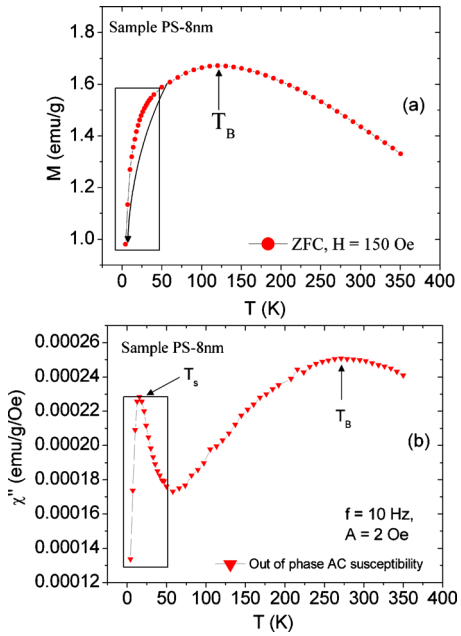


FIG. 4. (Color online) (a) ZFC curve under applied field H=150 Oe of sample *PS-8 nm*. Irregularity in low temperatures region is indicated by a rectangle. Arrow is drawn for a better look of *hump*, (b) Out-of-phase ac susceptibility of sample *PS-8 nm*. There is a peak in the low temperature region or hump region [as found in dc-ZFC susceptibility in Fig. 4(a)] as indicated by a rectangle.

=15 K. The in-phase $\chi'(T)$-plot (not shown here) shows the same hump in the low temperature region as it was found in dc-ZFC measurement in Fig. 4(a). The broad high temperature peak at 271 K is the average blocking temperature ($T_B$) of the magnetized core of the nanoparticles. Because the nanoparticles are dispersed in $SiO_2$ matrix (70%) in order to avoid interparticle interactions, the occurrence of the small peak at low temperature $T_s$=15 K is interpreted as a phase transition or freezing on the surface of *individual* particles.[15] Meneses *et al.*[16] has recently reported a similar low temperature peak in the out-of-phase ac susceptibility in NiO nanoparticles and attributed it to frustration and freezing of surface spins.

To investigate this effect of a surface spin-glass, we have tested the scaling law for sample *PS-8 nm* by measuring the frequency dependence of the ac susceptibility of the "spin-glass" peak as shown in Fig. 5. It shows a small peak shift from 13 to 19 K as the frequency is increased from 0.1 Hz to

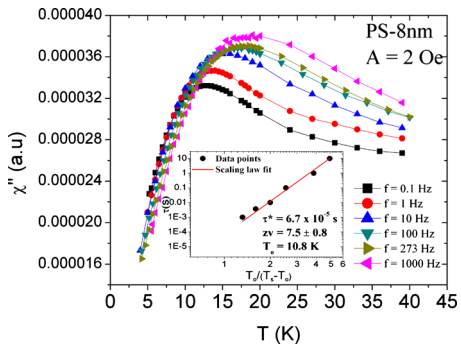


FIG. 5. (Color online) Frequency dependent ac susceptibility of the low temperature peak of sample *PS-8 nm*. Inset: Best fit of dynamic scaling law.

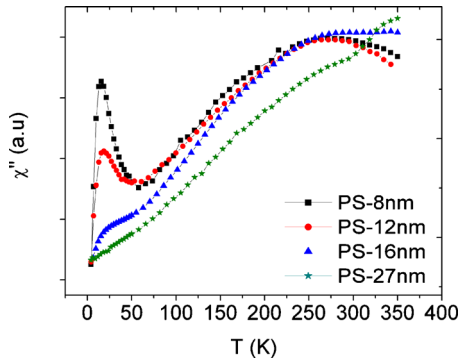


FIG. 6. (Color online) Out-of-phase ac susceptibility of different particle size samples *PS-8 nm*, *PS-12 nm*, *PS-16 nm*, and *PS-27 nm*. Note that the low temperature peak is vanishing on increasing particle size. Curves are shifted in vertical scale just for comparison.

1000 Hz, respectively. This frequency shift is fitted to a dynamic scaling law as defined in Ref. 17 and shown in the inset of Fig. 5:

$$\tau(f) = \tau^* \left[ \frac{T_o}{T_s(f) - T_o} \right]^{zv}. \quad (1)$$

In [Eq. (1)] $\tau(f)$ is the frequency dependent relaxation time of frozen spins, $\tau^*$ is related to the coherence time of coupled individual spins in the nanoparticle, $T_o$ is the "static" freezing temperature, "zv" the critical exponent (ranging from 4–12 for typical spin-glass systems[18,19]), and $T_s(f)$ is the frequency dependent freezing temperature as given by the maxima of the $\chi''(T)$-plots. Scaling law indicates that there is a critical slowing down of relaxation time near the transition temperature $T_o$. Best fit of the dynamic scaling law yields: $\tau^*=6.7\times10^{-5}$ s, $T_o$=10.8 K, and zv=7.5. The value of critical exponent zv fits to the expected spin-glass regime. The increased value of spin flip time $\tau^*$ is due to frozen agglomerates of highly disordered and frustrated surface spins which have a much longer relaxation time than individual spins in a spontaneously ordered bulk magnet with long-range magnon excitations ($\tau^*=10^{-9}-10^{-12}$ s).

We have also produced larger particles by reducing the $SiO_2$ matrix concentration. For larger particles we expect a sizeable interparticle dipolar interaction. Reduced concentration of the $SiO_2$ favors an increased particle size ranging up to 27 nm particles for a $SiO_2$ matrix concentration of 25%.[11] Figure 6 shows the out-of-phase ac susceptibility of samples *PS-8 nm*, *PS-12 nm*, *PS-16 nm*, and *PS-27 nm*. These plots demonstrate that the low temperature peak is vanishing upon increasing average particle diameter and is completely smeared out for sample *PS-27 nm*. The collapse of the low temperature peak for larger particles is attributed to the comparatively smaller contribution of surface spins in relation to its volume. In smaller sized particles, large concentration of $SiO_2$ matrix reduces the dipolar interactions among the nanoparticles, thus avoiding a possible superspin-glass freezing[20] (induced by interparticle dipolar interactions). This clearly indicates that the low temperature peak does not come about by superspin-glass freezing via interparticle dipolar interactions but is rather due to random freezing of disordered surface spins on the surface of *individual* nanoparticles.

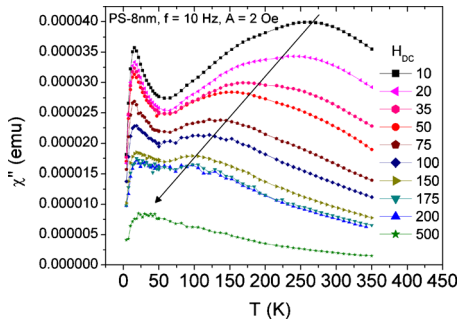


FIG. 7. (Color online) Out-of-phase ac susceptibility of sample *PS-8 nm* under external dc field (10–500 Oe). Arrow indicates the shift in the blocking peak with increasing dc field.

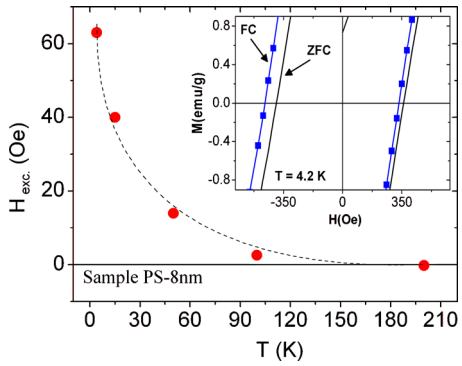


FIG. 8. (Color online) Temperature dependence of exchange bias ($H_{exc.}$) or horizontal hysteresis loop shift in sample *PS-8 nm*. Dotted line is just a trend indicator. Inset: detailed coercivity ($H_c$) region of ZFC (black line) and FC (blue rectangles connected with line) hysteresis loops measured at 4.2 K.

We have also checked the possibility of a bimodal particle size distribution in the smallest particle size sample *PS-8 nm*. In order to rule out a second low temperature freezing peak from a possible second particle size distribution, we have superimposed an external dc field in the ac susceptibility experiment. By superimposing an external dc field, one can reduce the anisotropy energy barriers between the opposite magnetized states of the nanoparticle. If the low temperature peak was due to blocking of nanoparticles with the smaller average particle size, then the low temperature peak of the ac susceptibility should shift *faster* than the high temperature peak (of the larger particle size) upon increasing the dc field. However, we have found an opposite (i.e., much less shift) behavior of the low temperature peak which is explained by the surface spin-glass freezing mechanism different from magnetic blocking effect of particles. Figure 7 shows the out-of-phase ac susceptibility of sample *PS-8 nm* at frequency f=10 Hz and amplitude A=2 Oe in external applied dc field ranging from 10–500 Oe. The magnetic blocking peak moves (see the arrow) toward lower temperature on increasing the dc field and finally collapses into the spin-glass peak. The anisotropy energy barrier of individual nanoparticle core spin is decreased with increasing dc field. Due to the lowering of the energy barrier with the applied dc field, less thermal energy is sufficient to overcome the barrier and hence blocking temperature is decreased with increasing dc field. However the spin-glass peak nearly maintains its position near T=15 K, instead it becomes solely damped with increasing external dc field. For a spin-glass system, there is a complicated landscape of irregularly distributed energy barriers instead of possessing a single well-defined energy barrier for magnetically blocked single domain particle.[8,21] The surface spins get trapped in the valleys of this energy landscape and require a comparatively strong dc field to surpass all these barriers. Thus we can also exclude any existence of a two-particle-size distribution in our matrix-protected samples. Superimposing dc field on the ac modulation field proves to be a good tool in distinguishing magnetic blocking and spin-glass freezing effects for nanoparticles.

Frozen surface spins strongly interact with core spins at low temperatures which is manifested by a field shift in the hysteresis loop called exchange bias ($H_{exc.}$) in nanoparticles.[6,7,22–24] Figure 8 shows the temperature dependence of the exchange bias ($H_{exc.}$) of sample *PS-8 nm*. For these measurements, we have first cooled the sample in field H=5 T to the desired low temperature and thereafter the hysteresis loop has been taken. Inset shows the detailed view of the coercivity region of two hysteresis loops measured at temperature T=4.2 K, first the reference hysteresis loop after ZFC (black line) and second the hysteresis loop taken after 5 T field cooling (FC) (blue rectangles connected with line). The FC loop shows an enhanced coercivity ($H_c$) and is slightly shifted toward the left side. This increase in coercivity ($H_c$) and shift in hysteresis loop under FC condition is due to the presence of competing interactions between aligned ferrimagnetic core and disordered surface spins.[7] Exchange bias ($H_{exc.}$) shows a sharp increase below 50 K due to freezing of the surface spins which interact strongly with the core spins at low temperatures. Exchange bias is nearly vanishing at 100 K due to quench of core-shell interactions caused by detachment of surface spins. Frozen surface spins also act as pinning centers on the surface of nanoparticles. Below 50 K, the coercivity ($H_c$) (not shown here) also shows a sharp increase which demonstrates an enhanced surface anisotropy due to freezing of random surface spins.[9,24] Martínez *et al.*[25] reported a sharp increase in exchange bias and coercivity at low temperatures in surface spin-glass maghemite nanoparticles.

We have also checked memory and aging effects which are more unique *fingerprints* for one of the samples, *PS-12 nm*, having surface spin-glass behavior. Memory effect in surface spin-glass nanoparticle systems is very difficult to measure experimentally because (i) the effect is very small in magnitude and (ii) the effect occurs in a very narrow temperature range below spin-glass freezing. In the memory experiment, a measuring protocol of two temperature scans is performed, one is the reference curve and the other is the memory curve (for which the system is halted below spin-glass temperature for some specific time). To get the reference curve, sample is ZFC from room temperature to 4.2 K in zero applied field and then ac susceptibility is recorded immediately on increasing temperature. For the memory curve, the sample is ZFC to the waiting temperature and halted there for some specific time (in our case 2 h). After this, the cooling is continued to 4.2 K and then ac suscepti-

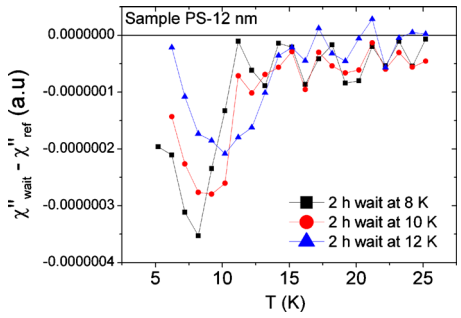


FIG. 9. (Color online) Difference of out-of-phase ac susceptibilities for the memory (when the system is halted at 8, 10, and 12 K for 2 h) and reference curve for sample *PS-12 nm*. Dip near 8 K, 10 K, and 12 K shows the memory effect at 8 K, 10 K, and 12 K, respectively. The dip shifts toward increasing temperature with increasing waiting temperature.

bility is recorded on increasing temperature.[26,27] Difference between the reference and memory curve indicates the presence of memory effect in the sample. Figure 9 shows the difference between the ac susceptibility memory (when the system is halted at 8, 10, and 12 K for 2 h) and the reference curve for sample *PS-12 nm*. For this experiment, we have measured out-of-phase ac susceptibility with frequency f =10 Hz and amplitude A=2 Oe. After subtracting the reference curve from the memory curve, a dip occurs near the waiting temperature, which demonstrates memory effect in the system.[28] The dip clearly shows a shift toward higher temperature and becomes damped with increasing waiting temperature. In the memory curve, magnetic moment decreases near the waiting temperature because the system remembers of its magnetic state at waiting temperature (which had nominally zero magnetic moment). At waiting temperature [8, 10, (or) 12 K], disorder among surface spins was increased due to increase in spin-glass correlation length among surface spins.

For aging experiment, first we have cooled the system in zero field from room temperature to 8 K. After halting for 0, 1, and for 2 h at 8 K, 50 Oe field is applied and the magnetic moment is measured as a function of time.[29] Figure 10 shows the aging experiment at temperature T=8 K with external applied dc field of 50 Oe after ZFC from room temperature for sample *PS-12 nm*. One can see that the aging curve of the magnetic moment amplitude decreases with increasing waiting time which clearly indicates aging effects in the system. The correlation among frozen surface spin-glass increases

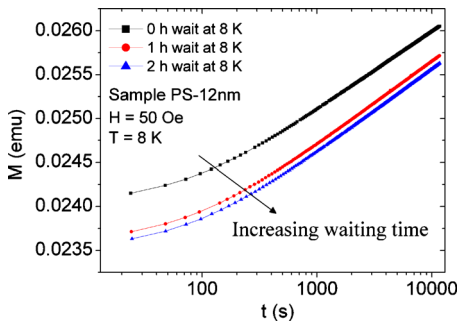


FIG. 10. (Color online) Waiting time (0, 1, and 2 h) dependence of magnetic moment at temperature T=8 K under field H=50 Oe after ZFC of sample *PS-12 nm*. Arrow indicates the trend of increasing waiting time.

with increase in waiting time, which in turn decreases the overall magnetic moment.

## IV. CONCLUSIONS

Magnetic properties of nickel ferrite nanoparticles dispersed in $SiO_2$ matrix have been discussed in detail. ZFC magnetization shows an anomalous behavior at low temperatures which is further investigated by ac susceptibility measurements. Out-of-phase ac susceptibility shows an extra peak at low temperature apart from the usual blocking peak at high temperature. The low temperature peak depends on the particle size and becomes suppressed upon increasing particle size. Particle diameter is increased by decreasing $SiO_2$ concentration or by increasing annealing time along with the preparation of the particles. Dipolar interactions among nanoparticles become important for a lowered concentration of the $SiO_2$ matrix but could be completely ruled out for our matrix-embedded particles. The nature of the existence of the low temperature peak in out-of-phase ac-susceptibility is further studied by frequency dependent ac susceptibility, dc field dependent ac susceptibility, exchange bias, coercivity, aging, and memory experiments. Dynamic scaling law fits the frequency dependent ac susceptibility of low temperature peak with critical exponent zv=7.5 which belongs to the spin-glass regime. dc field dependence of out-of-phase ac susceptibility shows a large shift in the blocking peak toward low temperatures with increasing dc field and finally collapses into the spin-glass peak, while the spin-glass peak shows nearly no shift but is only damped with increasing dc field. The rigidness of the spin-glass peak arises from the existence of irregular energy barriers which can be surpassed only by comparatively large external dc fields to quench the spin-glass behavior. While the shift in magnetic blocking peak is explained by a single energy barrier (with two potential minima) which is reduced upon increasing dc field and hence needs less thermal energy to be overcome. Temperature dependent exchange bias ($H_{exc.}$) shows a sharp increase at low temperatures due to presence of core-shell interactions at low temperatures. Aging and memory experiments also signify the existence of spin-glass behavior in these nanoparticles. The memory dip shifts toward higher temperature and becomes damped with increasing waiting temperature. The spin-glass behavior in nanoparticles may arise either from the random freezing of the nanoparticles due to dipolar interactions or due to surface spin freezing on the surface of individual nanoparticles. The collapse of the low temperature "spin-glass" peak upon increasing the particle diameter excludes the possibility of superspin-glass formation which can occur only due to interparticle dipolar interactions. Hence the preparation of $SiO_2$-embedded Ni-ferrite nanoparticles rules out superspin glass phase in favor of surface spin-glass freezing.

## ACKNOWLEDGMENTS

K. Nadeem acknowledges the Higher Education Commission (HEC) of Pakistan for providing foreign Ph.D. scholarship. The authors also thank the Austrian Science

Fund (FWF) (national funds) for granting the network projects (NFN) S10407-N16, S10405-N16, and the NAWI-Graz GASS cooperation project.

[1]D. Fiorani, A. M. Testa, F. Lucari, F. D'Orazio, and H. Romero, Physica B **320**, 122 (2002).
[2]S. Linderoth, P. V. Hendriksen, F. Bødker, S. Wells, K. Davis, S. W. Charles, and S. Mørup, J. Appl. Phys. **75**, 6583 (1994).
[3]S. Mørup, Europhys. Lett. **28**, 671 (1994).
[4]*Surface Effects in Magnetic Nanoparticles*, 1st ed., edited by D. Fiorani (Springer, New York, 2005).
[5]S. Middey, S. Jana, and S. Ray, J. Appl. Phys. **108**, 043918 (2010).
[6]R. H. Kodama and A. E. Berkowitz, Phys. Rev. B **59**, 6321 (1999).
[7]R. H. Kodama, A. E. Berkowitz, E. J. McNiff, and S. Foner, Phys. Rev. Lett. **77**, 394 (1996).
[8]K. Binder and A. P. Young, Rev. Mod. Phys. **58**, 801 (1986).
[9]E. Winkler, R. D. Zysler, M. Vasquez Mansilla, D. Fiorani, D. Rinaldi, M. Vasilakaki, and K. N. Trohidou, Nanotechnology **19**, 185702 (2008).
[10]D. Peddis, C. Cannas, G. Piccaluga, E. Agostinelli, and D. Fiorani, Nanotechnology **21**, 125705 (2010).
[11]K. Nadeem, T. Traussnig, I. Letofsky-Papst, H. Krenn, U. Brossmann, and R. Würschum, J. Alloys Compd. **493**, 385 (2010).
[12]J. Smit and H. P. J. Wijn, *Ferrites-Physical Properties of Ferromagnetic Oxides in Relation to Their Technical Applications* (Wiley, New York, 1959).
[13]A. Kale, S. Gubbala, and R. D. K. Misra, J. Magn. Magn. Mater. **277**, 350 (2004).
[14]K. Nadeem and H. Krenn, *Functional Oxide Nanostructures and Heterostructures*, MRS Symposia Proceedings Vol. 1256E (Materials Research Society, Pittsburgh, 2010), p. N06-06.
[15]R. J. Tackett, A. W. Bhuiya, and C. E. Botez, Nanotechnology **20**, 445705 (2009).
[16]C. T. Meneses, J. G. S. Duque, E. de Biasi, W. C. Nunes, S. K. Sharma, and M. Knobel, J. Appl. Phys. **108**, 013909 (2010).
[17]P. C. Hohenberg and B. I. Halperin, Rev. Mod. Phys. **49**, 435 (1977).
[18]J. A. Mydosh, *Spin Glasses* (Taylor & Francis, Washington, 1993).
[19]K. H. Fischer and J. A. Hertz, *Spin Glasses* (Cambridge University Press, Cambridge, 1991).
[20]D. Parker, V. Dupuis, F. Ladieu, J. P. Bouchaud, E. Dubois, R. Perzynski, and E. Vincent, Phys. Rev. B **77**, 104428 (2008).
[21]G. C. Papaefthymiou, Nanotoday **4**, 438 (2009).
[22]C. N. Chinnasamy, A. Narayanasamy, N. Ponpandian, R. J. Joseyphus, B. Jeyadevan, K. Tohji, and K. Chattopadhyay, J. Magn. Magn. Mater. **238**, 281 (2002).
[23]J. Nogués, J. Sort, V. Langlais, V. Skumryev, S. Suriñach, J. S. Muñoz, and M. D. Baró, Phys. Rep. **422**, 65 (2005).
[24]M. Kiwi, J. Magn. Magn. Mater. **234**, 584 (2001).
[25]B. Martínez, X. Obradors, L. Balcells, A. Rouanet, and C. Monty, Phys. Rev. Lett. **80**, 181 (1998).
[26]P. Jönsson, M. F. Hansen, and P. Nordblad, Phys. Rev. B **61**, 1261 (2000).
[27]K. Nadeem and H. Krenn, "Exchange Bias, Memory and Freezing Effects in $NiFe_2O_4$ Nanoparticles," J. Supercond. Novel Magn.
[28]M. Sasaki, P. E. Jönsson, H. Takayama, and H. Mamiya, Phys. Rev. B **71**, 104405 (2005).
[29]V. Bisht and K. P. Rajeev, J. Phys.: Condens. Matter **22**, 016003 (2010).